

Open-loop temperature control for a distributed parameter model of a pipe

Simon Bachler* Jens Wurm* Frank Woittennek*

* Institute of Automation and Control Engineering,
 UMIT - Private University for Health Sciences, Medical Informatics
 and Technology, Eduard Wallnöfer Zentrum 1, Hall in Tirol, Austria
 (e-mail: {simon.bachler, jens.wurm, frank.woittennek}@umit.at)

Abstract: Various models describing a plug flow through a pipe are used for model-based control design in industrial processes. This contribution presents a feedforward controller based on a new modeling approach for plug flow through a pipe. The latter model combines the advantages of partial differential and delay differential equation approaches. This structure allows to derive the desired control input by an inverse calculation of the partial differential equation part of the model. Moreover, the stability of the used model is proven by a spectrum analysis of the involved system operators. Finally, the presented approach is studied in simulation and experimentally test results are provided.

Keywords: flow control, delay differential equation, partial differential equation, distributed parameter system, hyperbolic equation, transport delay.

1. INTRODUCTION

Plug flow models are widely used in industrial environments, like solar desalination plants (Santos et al., 2011), district heating grids (Jie et al., 2012), cooling loops of large gas engines (Bachler et al., 2017a), and Diesel oxidation catalysts (Lepreux, 2009). Therein different sophisticated control strategies are used. For instance the output temperature is controlled by an adaptive control law, based on a discretized thermal partial differential equation (PDE) or a delay differential equation (DDE) model. Lemos (2006) presents a significant example for this type of work. Moreover, Lepreux et al. (2008) introduces an open-loop control concept by an inversion of the inlet-to-outlet temperature transfer function for a Diesel oxidation catalyst. The current contribution presents a different view on these latter results from a state-space perspective. As the above cited references it is based on the standard PDE thermal pipe model, which includes the transport phenomena in combination with the heat exchange between fluid and wall respectively wall and ambient. It relies on a reformulation of this model as an interconnection of a pure delay system and another PDE model proposed in Bachler et al. (2017a) and Wurm et al. (2020). In accordance with these references the latter model is called delay partial differential equation (DPDE) model. The specific structure of the DPDE allows for a backward calculation, which makes a simple calculation of the feedforward law possible. In contrast to the control law presented by Lepreux et al. (2008) no convolution operations have to be performed. Moreover, the DPDE model allows an extension for variable flow rates.

The remaining part of the contribution is structured as follows: The standard pipe model is introduced in Section 2. The main results concerning the control design are collected in Section 3. This includes the derivation of

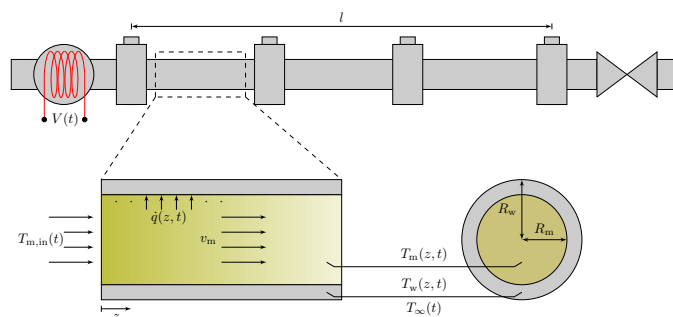


Fig. 1. Sketch of pipe test rig and used variables.

the DPDE model and the corresponding inverse model in Section 3.1, the well-posedness and stability analysis in Section 3.2, and the numerical implementation of the control design in Section 3.3. Finally, simulation studies and experimental results are presented in Section 4.

2. MODELING

The thermal behavior of a plug flow in a long pipe can be described in various ways. For instance PDE models are used if spatial distributed temperature information is required. In contrast DDE or ordinary differential equation (ODE) models are used when small calculation times are needed. Within this section the common PDE model is presented. Fig. 1 depicts the considered pipe of length l with inner and outer radii R_m and R_w . The temperatures of the medium, the wall, and the ambient are denoted by T_m , T_w , and T_∞ , respectively. The inflow temperature $T_{m,in}$ is adjusted by a heater which is controlled by the input voltage V . The velocity of the medium is denoted by v_m while the heat flux between medium, wall and ambient is \dot{q} . For the modeling an (i) incompressible medium with (ii) a radially constant temperature and velocity profile

due to turbulent flow regime is assumed. Furthermore, thanks to a sufficiently large (iii) constant medium velocity (iv) the thermal conduction in flow direction is neglected for both, the wall and the medium, and (v) all material parameters are assumed to be constant w.r.t. both space and time. For the modeling the pipe depicted in Fig. 1 can be split up into a medium and a wall part, which are treated separately in the next subsections.

2.1 Medium

Taking into account Assumption (ii), a constant temperature profile over the cross section of the medium can be assumed. Assumption (iv) leads to the well known one-dimensional transport equation describing the fluid flow in z -direction:

$$A_m c_{p,m} \rho_m (v_m \partial_z T_m(z, t) + \partial_t T_m(z, t)) = -U_m \dot{q}(R_m, z, t) \quad (1a)$$

with the specific heat capacity $c_{p,m}$, the density ρ_m , the cross-section area A_m , and the inner circumference U_m of the pipe. The heat flux $\dot{q}(R_m, z, t)$ from the medium into the wall can be described by

$$-\dot{q}(R_m, z, t) = \alpha_{mw} (T_w(z, t) - T_m(z, t)) \quad (1b)$$

with the heat transfer coefficient α_{mw} between medium and wall (cf. Baehr and Stephan, 2011). The initial condition and the corresponding inflow boundary condition are

$$T_m(0, t) = T_{m,in}(t), \quad T_m(z, 0) = T_{m,0}(z), \quad (1c)$$

respectively, with the input temperature $T_{m,in}$ and the initial temperature profile $z \mapsto T_{m,0}(z)$.

2.2 Wall

Neglecting the heat flux in axial direction in view of Assumption (iii) the temperature distribution within the jacket can be described by

$$A_w \rho_w c_{p,w} \partial_t T_w(z, t) = U_m \dot{q}(R_m, z, t) - U_w \dot{q}(R_w, z, t) \quad (2a)$$

with the heat flux $\dot{q}(R_m, z, t)$ between medium and wall according to (1b) and the heat flux $\dot{q}(R_w, z, t)$ between wall and ambient given by

$$-\dot{q}(R_w, z, t) = -\alpha_{wa} (T_w(z, t) - T_\infty(t)). \quad (2b)$$

In above equations α_{wa} denotes the heat transfer coefficient between wall and ambient, A_w the cross-sectional area, and U_w the circumference of the wall. The initial condition is

$$T_w(z, 0) = T_{w,0}(z). \quad (2c)$$

2.3 Overall PDE model

An overall one-dimensional model can be obtained by (1) and (2), which results in the one-dimensional PDE system

$$v_m \partial_z T_m(z, t) + \partial_t T_m(z, t) = h_1 (T_w(z, t) - T_m(z, t)) \quad (3a)$$

$$\begin{aligned} \partial_t T_w(z, t) &= h_2 (T_m(z, t) - T_w(z, t)) \\ &\quad - h_3 (T_w(z, t) - T_\infty(t)) \end{aligned} \quad (3b)$$

with boundary condition

$$T_m(0, t) = T_{m,in}(t) \quad (3c)$$

and the initial conditions

$$T_m(z, 0) = T_{m,0}(z), \quad T_w(z, 0) = T_{w,0}(z). \quad (3d)$$

The physical parameters are collected in the coefficients

$$h_1 = \frac{U_m}{A_m} \frac{\alpha_{mw}}{\rho_m c_{p,m}}, \quad h_2 = \frac{U_m}{A_w} \frac{\alpha_{mw}}{\rho_w c_{p,w}}, \quad h_3 = \frac{U_w}{A_w} \frac{\alpha_{wa}}{\rho_w c_{p,w}}.$$

As illustrated in Fig. 1 a flow heater is installed at the inlet of the pipe to reach a desired input temperature evolution $\hat{T}_{m,in}$. The power of the heater can be controlled by the input voltage V . In a first step, the inlet temperature is assumed to be perfectly adjusted by the heater. The control strategy for the heater is not further emphasized in the following considerations.

3. FEEDFORWARD CONTROL

In this section an open-loop control approach for tracking a desired outflow temperature is presented. Based on the model equations (3) the corresponding input temperature trajectory $t \mapsto T_{m,in}(t)$ has to be determined. However, the associated inverse model, which is constituted by (3) with boundary condition at $z = l$ instead of 0 and initial conditions (3d) is easily shown to be ill posed. As a consequence this inverse model has to be formulated in a different way: This is achieved by separating the transport delay from the model equations (3). According to Sec. 3.2 the remaining delay free model (cf. Bachler et al., 2017b; Wurm et al., 2020), which is called DPDE model in the sequel, can then be easily inverted by interchanging the role of the input and the output. In order to numerically compute the open-loop control signal an approximation of the introduced inverse DPDE model is used.¹

3.1 Derivation of the DPDE model

Evaluating the medium part (3a) of the overall PDE model on its characteristic curves (cf. Courant and Hilbert, 1962; John, 1991)

$$\Gamma : \xi \mapsto (z, t) = (z(\xi), t(\xi)), \quad \xi \in \mathbb{R}$$

defined by

$$\frac{dz}{d\xi}(\xi) = 1, \quad \frac{dt}{d\xi}(\xi) = \frac{1}{v_m} \quad (4)$$

yields

$$\frac{dT_m}{d\xi}(z(\xi), t(\xi)) = \frac{h_1}{v_m} (T_w(z(\xi), t(\xi)) - T_m(z(\xi), t(\xi))).$$

For $z \in [0, l]$, $z(0) = 0$, and $t(l) = \bar{t}$ one obtains from (4) $z = \xi$ and

$$t(z) = \bar{t} - \tau(l - z) = \varphi(z, \bar{t}), \quad \tau(z) = \frac{z}{v_m},$$

which can be interpreted as a space dependent time delay. Note that in the following \bar{t} is replaced by t for convenience.

Introducing the delayed temperature

$$T_\bullet^{\text{del}}(z, t) = T_\bullet(z, t - \tau(l - z)) = T_\bullet(z, \varphi(z, t))$$

¹ As already stated within the introduction the proposed approach can be seen as a state-space interpretation of the results presented in Lepreux et al. (2008). Note that apart from the differences in the formulation and the completely different numerical implementation the model is extended by the ambient temperature in the current contribution.

and its derivatives

$$\begin{aligned}\partial_t T_{\bullet}^{\text{del}}(z, t) &= \partial_{\varphi} T_{\bullet}(z, \varphi(z, t)) \\ \partial_z T_{\bullet}^{\text{del}}(z, t) &= \partial_z T_{\bullet}(z, \varphi(z, t)) + \frac{1}{v_m} \partial_{\varphi} T_{\bullet}(z, \varphi(z, t)),\end{aligned}$$

where \bullet may be replaced by m, w, ∞ , the one-dimensional model (3) can be rewritten to

$$v_m \partial_z T_m^{\text{del}}(z, t) = h_1 (T_w^{\text{del}}(z, t) - T_m^{\text{del}}(z, t)) \quad (5a)$$

$$\begin{aligned}\partial_t T_w^{\text{del}}(z, t) &= h_2 (T_m^{\text{del}}(z, t) - T_w^{\text{del}}(z, t)) \\ &+ h_3 (T_{\infty}^{\text{del}}(z, t) - T_w^{\text{del}}(z, t)).\end{aligned} \quad (5b)$$

Note that a variable flow rate leads to an time dependent delay, which has to be considered when calculating the derivatives of the delayed temperatures (cf. Wurm et al., 2020).

Solving (5a) for T_w^{del} and substituting the result into (5b) reveals

$$\begin{aligned}\partial_t T_m^{\text{del}}(z, t) + \frac{h_1}{v_m} \partial_t T_m^{\text{del}}(z, t) + \frac{h_1 h_3}{v_m} T_m^{\text{del}}(z, t) \\ + (h_2 + h_3) \partial_z T_m^{\text{del}}(z, t) = \frac{h_1 h_3}{v_m} T_{\infty}^{\text{del}}(z, t)\end{aligned} \quad (6a)$$

with the boundary condition

$$T_m^{\text{del}}(0, t) = T_{m,\text{in}}^{\text{del}}(t) = T_{m,\text{in}}(t - \tau(l)) \quad (6b)$$

and the output equation

$$T_{m,\text{out}}(t) = T_m^{\text{del}}(l, t) = T_{m,\text{out}}^{\text{del}}(t). \quad (6c)$$

According to Bachler et al. (2017b) and Wurm et al. (2020) the latter model is called DPDE model.

For the control design the inverse of the above DPDE model is employed, which is obtained by interchanging the meaning of the inflow boundary condition (6b) and the output equation (6c). As a consequence the inverse DPDE model is given by (6a) with the boundary condition

$$T_m^{\text{del}}(l, t) = T_{m,\text{out}}^{\text{del}}(t) = T_{m,\text{out}}(t) \quad (7a)$$

and the output equation

$$T_{m,\text{in}}(t - \tau(l)) = T_m^{\text{del}}(0, t) = T_{m,\text{in}}^{\text{del}}(t). \quad (7b)$$

To compute the feedforward control (6a) and (7) are solved for a prescribed predicted outflow temperature

$$T_{m,\text{out}}^{\text{pred}}(t) = T_{m,\text{out}}^{\text{del}}(t + \tau(l)) = T_{m,\text{out}}(t + \tau(l)).$$

Finally, the corresponding inflow temperature $T_{m,\text{in}}(t) = T_{m,\text{in}}^{\text{pred}}(t)$ can be read off from (7b). Note that the prediction of the reference trajectory is needed in order to compensate for the delay occurring in (7b).

3.2 Stability of the (inverse) DPDE model

For applicability of the proposed control design stability of the inverse DPDE model is required. Note that the stability properties of the original (6) and the inverse model (6a), (7) coincide and can be shown in the same way. Thus, within this section only the stability of the original model (6) is investigated.

To cancel the pure time derivative of the medium temperature in (6a), the transformation

$$T_m^{\text{del}}(z, t) = e^{-\frac{h_1}{v_m} z} \bar{T}_m^{\text{del}}(z, t)$$

is introduced. Hence, (6a) changes to

$$\begin{aligned}\partial_t z \bar{T}_m^{\text{del}}(z, t) + (h_2 + h_3) \partial_z \bar{T}_m^{\text{del}}(z, t) \\ - \frac{h_1 h_2}{v_m} \bar{T}_m^{\text{del}}(z, t) = d(z) T_{\infty}^{\text{del}}(z, t)\end{aligned} \quad (8)$$

with the spatial coefficient $d(z) = \exp\left(\frac{h_1}{v_m} z\right) \frac{h_1 h_3}{v_m}$. An integration of (8) w.r.t. z leads to

$$\begin{aligned}\partial_t \bar{T}_m^{\text{del}}(z, t) - \partial_t \bar{T}_m^{\text{del}}(0, t) + (h_2 + h_3) (\bar{T}_m^{\text{del}}(z, t) - \bar{T}_m^{\text{del}}(0, t)) \\ - \frac{h_1 h_2}{v_m} \int_0^z \bar{T}_m^{\text{del}}(\zeta, t) d\zeta = \int_0^z d(\zeta) T_{\infty}^{\text{del}}(\zeta, t) d\zeta.\end{aligned}$$

The state $x(\cdot, t) = \bar{T}_m^{\text{del}}(\cdot, t) - \bar{T}_{m,\text{in}}^{\text{del}}(t) \in X = \mathbf{L}_2[0, l]$ is introduced, where \mathbf{L}_2 denotes the space of square-integrable functions. This way the latter equation can be rewritten in the form

$$d_t x(\cdot, t) = \mathcal{A}x(\cdot, t) + \mathcal{B}u(\cdot, t) \quad (9a)$$

with the system bounded operator $\mathcal{A} : X \rightarrow X$

$$\mathcal{A}\bar{x} = -(h_2 + h_3)\bar{x} + \frac{h_1 h_2}{v_m} \mathcal{V}(\bar{x}), \quad \bar{x} \in X \quad (9b)$$

and the bounded input operator $\mathcal{B} : \mathbb{R}^2 \rightarrow X$

$$(\mathcal{B}u(t))(z) = \frac{h_1 h_2}{v_m} z \bar{T}_{m,\text{in}}^{\text{del}}(t) + \int_0^z d(\zeta) T_{\infty}^{\text{del}}(\zeta, t) d\zeta. \quad (9c)$$

Additionally, the Volterra operator in (9b) is defined by $\mathcal{V}(\bar{x})(z) = \int_0^z \bar{x}(\zeta) d\zeta$. The ambient temperature T_{∞}^{del} and the boundary value $\bar{T}_{m,\text{in}}^{\text{del}}$ are considered as inputs and are collected in $u \in \mathbb{R}^2$.

Since \mathcal{A} is bounded it is the infinitesimal generator of the uniformly continuous C_0 -semigroup as described in (Pazy, 1983, Theorem 1.2). As a consequence, the spectrum σ of the system operator completely determines the stability properties of the generated semigroup (see Engel, 1999, Theorem I.3.14).

At first the injectivity of $sI - \mathcal{A}$, $s \in \mathbb{C}$, is checked by solving

$$(sI - \mathcal{A})\bar{x} = 0,$$

i.e.

$$(s + h_2 + h_3)\bar{x}(z) - \frac{h_1 h_2}{v_m} \int_0^z \bar{x}(\zeta) d\zeta = 0. \quad (10)$$

A spatial differentiation of (10) reveals

$$(s + h_2 + h_3) \partial_z \bar{x}(z) - \frac{h_1 h_2}{v_m} \bar{x}(z) = 0. \quad (11)$$

One can easily see that the cases (a) $s = -h_2 - h_3$ and (b) $s \neq -h_2 - h_3$ have to be studied separately.

(a) For the case that $s = -h_2 - h_3$ (11) implies

$$-\frac{h_1 h_2}{v_m} \bar{x}(z) = 0$$

and therefore, $\bar{x} = 0$.

(b) Assuming $s \neq -h_2 - h_3$ one can solve (11) to obtain

$$\bar{x}(z) = \bar{x}(0) \exp\left(\frac{h_1 h_2}{v_m (s + h_2 + h_3)} z\right), \quad (12)$$

which again yields the trivial solution $\bar{x}(z) = 0$ after applying the boundary value $\bar{x}(0) = 0$ complying with

(10). Consequently, $sI - \mathcal{A}$ is injective independently of s . Thus, there are no eigenvalues and the point spectrum σ_p of the system operator is empty:

$$\sigma_p(\mathcal{A}) = \emptyset.$$

In a second step surjectivity of $sI - \mathcal{A}$ is examined by analyzing $(sI - \mathcal{A})\bar{x} = \bar{y}$, i.e.,

$$(s + h_2 + h_3)\bar{x}(z) - \frac{h_1 h_2}{v_m} \int_0^z \bar{x}(\zeta) d\zeta = \bar{y}(z). \quad (13)$$

(a) In the case $s = -h_2 - h_3$ spatial differentiation of (13) delivers

$$\bar{x}(z) = -\frac{v_m}{h_1 h_2} \partial_z \bar{y}(z).$$

As a consequence, the range of $sI - \mathcal{A}$ equals $\mathcal{H}_1[0, l] \subset \mathbf{L}_2[0, l]$, where $\mathcal{H}_1[0, l]$ denotes the Sobolev space of (weakly) differentiable functions in $\mathbf{L}_2[0, l]$: The operator $sI - \mathcal{A}$ is not surjective for $s = -h_2 - h_3$ but has a dense image. Thus, $s = -h_2 - h_3$ belongs to continuous spectrum of \mathcal{A} (Curtain and Zwart, 1995).

(b) Again, assuming $s \neq -h_2 - h_3$ by evaluating a spatial differentiation of (13) leads to

$$\partial_z \bar{x}(z) - \frac{h_1 h_2}{v_m(s + h_2 + h_3)} \bar{x}(z) = \frac{\partial_z \bar{y}(z)}{s + h_2 + h_3}$$

with initial conditions $\bar{x}(0) = \bar{y}(0)$. Using the standard variation of constants solution for this inhomogeneous ODE together with the initial condition, a simple integration by parts reveals the solution of the latter equation and, therefore, of (13):

$$\bar{x}(z) = \frac{\bar{y}(z)}{\nu} - \frac{h_1 h_2}{v_m \nu^2} \int_0^z e^{\frac{h_1 h_2}{v_m \nu}(z-\zeta)} \bar{y}(\zeta) d\zeta.$$

Therein, $\nu = s + h_2 + h_3 \neq 0$. Since the right-hand side of the above solution defines a bounded linear map on $\mathbf{L}_2[0, l]$, $sI - \mathcal{A}$ is surjective for all $s \neq -h_2 - h_3$.

Summarizing the above analysis, the spectrum of \mathcal{A} consists of the continuous spectrum only (Curtain and Zwart, 1995):

$$\sigma_c(\mathcal{A}) = \{-h_2 - h_3\}.$$

Thus the following theorem holds.

Theorem 1. The operator \mathcal{A} defined in (9b) generates an uniformly continuous and exponentially stable semigroup (Engel, 1999, Theorem I.3.14) satisfying

$$\|e^{\mathcal{A}t}\| \leq C e^{-\mu t}, \quad \forall \mu < h_2 + h_3$$

and an appropriate positive constant C , depending on μ . Moreover, \mathcal{B} is continuous the solution

$$x(\cdot, t) = e^{\mathcal{A}t} x(\cdot, 0) + \int_0^t e^{\mathcal{A}(t-\tau)} \mathcal{B}u(\cdot, \tau) d\tau$$

is well defined and bounded for bounded inputs.

Proof. Since \mathcal{A} is bounded it generates a uniformly continuous semigroup satisfying the spectrum determined growth condition. By the above analysis and the boundedness of \mathcal{B} the result is an immediate consequence of (Engel, 1999, Theorem I.3.4).

3.3 Numerical Implementation

In order to calculate the open-loop inflow temperature $T_{m,\text{in}}$ from a predicted prescribed output temperature $T_{m,\text{out}}^{\text{pred}}$ the DPDE model is discretized w.r.t. the spatial variable. This is achieved by means of the finite difference method (FDM), i.e., by approximating the spatial derivatives by the difference $(T_{\bullet,i}(t) := T_{\bullet}^{\text{del}}(z_i, t))$:

$$(\partial_z T_{\bullet}^{\text{del}})(z_i, t) \approx \frac{T_{\bullet,i}(t) - T_{\bullet,i-1}(t)}{\Delta z}, \quad i = 1, \dots, n.$$

Therein, n specifies the number of $n + 1$ equidistant sampling points z_0, \dots, z_n with the distance $\Delta z = l/n$. As a consequence the DPDE model (6) can be approximated by a system of n ODEs:

$$d_t (T_{m,i-1}(t) - k_1 T_{m,i}(t)) = k_2 (T_{m,i}(t) - T_{m,i-1}(t)) + k_3 (T_{\infty,i}(t) + T_{m,i}(t)) \quad (14)$$

with the constants

$$k_1 = \frac{v_m + h_1 \Delta z}{v_m}, \quad k_2 = h_2 + h_3, \quad k_3 = \frac{h_1 h_3 \Delta z}{v_m}.$$

In order to derive the feedforward signal, the DPDE approximation (14) can be represented by the matrix equation

$$d_t \mathbf{T}_m(t) = \mathbf{A}_m \mathbf{T}_m(t) + \mathbf{b}_{m,1} d_t T_{m,\text{out}}(t) + \mathbf{b}_{m,2} T_{m,\text{out}}(t) + \mathbf{D}_m \mathbf{T}_{\infty}(t) \quad (15)$$

with the corresponding system matrix $\mathbf{A}_m \in \mathbb{R}^{n \times n}$, input vectors $\mathbf{b}_{m,1}, \mathbf{b}_{m,2} \in \mathbb{R}^n$, and disturbance matrix $\mathbf{D}_m \in \mathbb{R}^{n \times n}$. The delayed temperatures are collected in

$$\mathbf{T}_{\bullet}(t) = (T_{\bullet,0}(t), T_{\bullet,2}(t), \dots, T_{\bullet,n-1}(t))^T.$$

In order to obtain a continuous input temperature

$$T_{m,\text{in}}^{\text{pred}}(t) = T_{m,0}(t) = T_{m,\text{in}}(t) = T_{m,\text{in}}^{\text{del}}(t + \tau(l)),$$

the prescribed output temperature $T_{m,\text{out}}^{\text{pred}}$ has to be at least continuous. To obtain a smooth transition the prescribed outflow temperature is defined by the trajectory:

$$T_{m,\text{out}}^{\text{pred}}(t) = \begin{cases} T_{m,\text{out},S}, & t \leq t_S \\ 3 \frac{(t-t_S)^2}{\Delta t^2} - 2 \frac{(t-t_S)^3}{\Delta t^3}, & t_S < t < t_E \\ T_{m,\text{out},E}, & t \geq t_E. \end{cases} \quad (16)$$

The planned trajectory starts at time t_S from the initial output temperature $T_{m,\text{out},S}$ and ends at the final output temperature $T_{m,\text{out},E}$ at time t_E . Therein, the transition time is denoted by $\Delta t = t_E - t_S$.

Note that in case of variable flow the previously described steps can be applied in a similar way.

4. SIMULATION STUDY AND EXPERIMENTAL VALIDATION

In this section the feedforward control approach is verified in simulation studies and validated experimentally on the test rig depicted in Fig. 2. This test rig was specifically designed for validation of various numerical approximations of the DPDE model proposed in Wurm et al. (2020). An extended version of this test rig is used to show the applicability of the presented feedforward control approach. All further investigations consider the medium to be water. The pipe under consideration has a total length of 5.54 m, an inner diameter of 16.2 mm and an outer diameter of 22 mm. At nine measurement

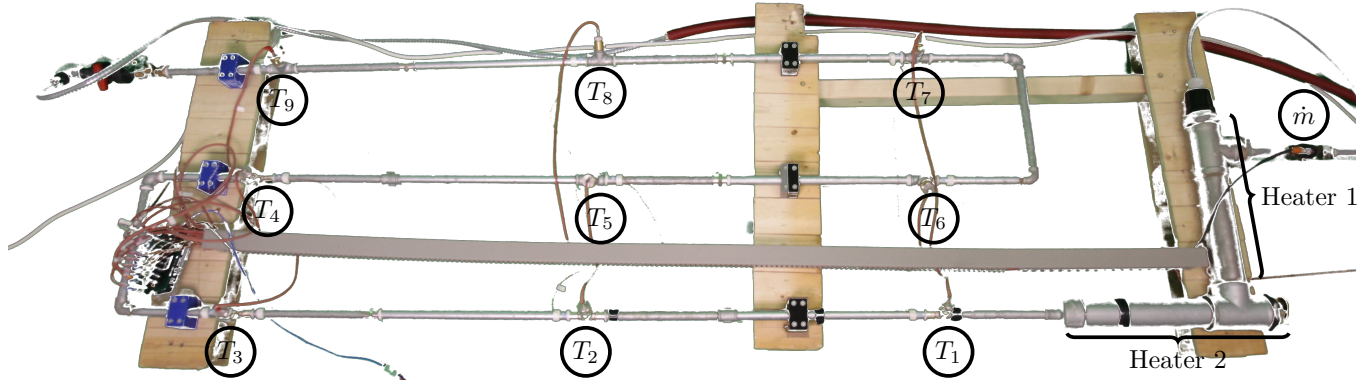


Fig. 2. Pipe test rig used for validation of the control strategy.

Table 1. Used parameters for studies.

Parameter	Value	Unit
ρ_w	7856	$\frac{\text{kg}}{\text{m}^3}$
$c_{p,w}$	500	$\frac{\text{J}}{\text{kg K}}$
ρ_m	997.04	$\frac{\text{kg}}{\text{m}^3}$
$c_{p,m}$	4179	$\frac{\text{J}}{\text{kg K}}$
l	5.54	m
α_{mw}	3032.16	$\frac{\text{W}}{\text{m}^2 \text{K}}$
α_{wa}	67.22	$\frac{\text{W}}{\text{m}^2 \text{K}}$

points, which are distributed over the entire length (cf. Fig. 2), the medium and wall temperatures are captured by PT100 and thermocouples, respectively. Additionally, the ambient temperature is measured by another thermocouple while the volume flow rate through the pipe is tracked by applying the principle of differential pressure. The heater has a total power of 9 kW and is controlled by pulse width modulation (PWM) triggering a thyristor relay. The medium temperature before the heater is also captured by a PT100 sensor. The signal processing and control of the heater PWM signal is done by an Arduino Mega complemented with appropriate sensor boards. The required heat transfer coefficients α_{mw} and α_{wa} of the pipe are determined by a least squares identification algorithm based on the measured medium temperature at the in- and outlet. The simulation study and validation are performed in Python. Tab. 1 presents the used physical parameters for the DPDE model (6) and for the benchmark model (3).

4.1 Simulation study

For the simulation study the following scenario is considered: a polynomial temperature trajectory as defined in (16) is prescribed at the output $z = l$ of the pipe. It starts at 13 °C and ends at 65 °C after a transition time of 150 s. The medium velocity is set to 0.8 $\frac{\text{m}}{\text{s}}$ and an ambient temperature of 25 °C is assumed. For the scenario the discretized feedforward controller (15) is used with $n = 4$. The derived control law from (15) is feed to a by the FDM discretized one-dimensional PDE model (3) with an high resolution of 201 sampling points. The results of these simulation are presented in Fig. 3. One can easily see

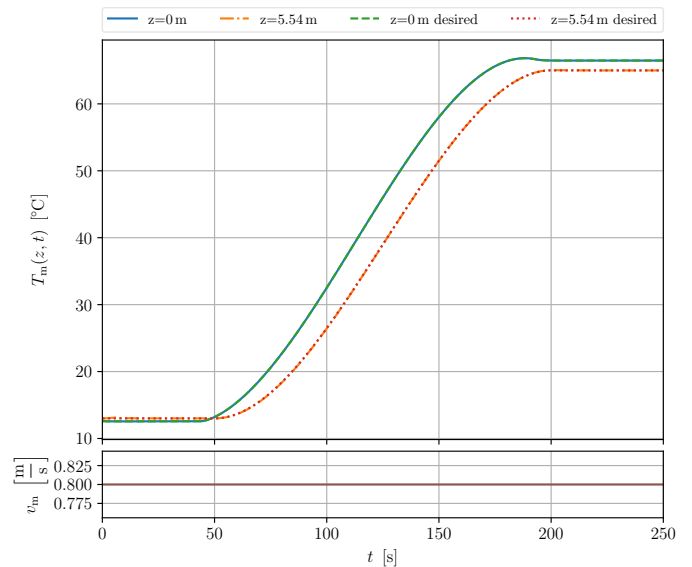


Fig. 3. Simulation results of presented feedforward control approach.

that the desired output temperature is perfectly tracked by the feedforward controller.

4.2 Measurement study

For the measurement study a polynomial transition of the form (16) is planned for the desired pipe outlet temperature $T_{m,out}^{pred}$. A transition from 20 °C to 35 °C in 150 s is intended. To this end, the desired input temperature $T_{m,in}^{pred}$ is calculated by applying (15) with $n = 4$. Moreover, a constant ambient temperature of 26 °C and a constant velocity of 0.42 $\frac{\text{m}}{\text{s}}$ is assumed to derive $T_{m,in}^{pred}(t) = T_{m,in}(t)$. In order to track the desired input temperature a proportional–integral–derivative (PID) controller combined with a Smith predictor (Smith, 1957) is implemented at the Arduino board. The Smith predictor is based on a simple linear heater model, approximating the heater dynamics for a certain velocity and ambient temperature. As Fig. 4 illustrates, the desired input temperature cannot be perfectly pursued by the heater controller. This is mainly caused by the simple heater model used for the Smith predictor. Nevertheless, it can be seen that the measured outlet temperature nearly meets the desired one.

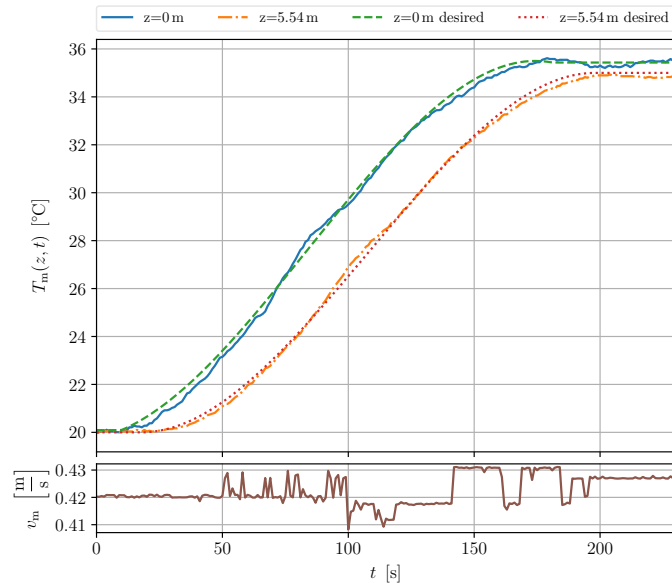


Fig. 4. Measurement data compared against desired values at the pipe out- and inlet.

5. CONCLUSION AND OUTLOOK

The contribution presents a feedforward control approach for a plug flow through a pipe based on distributed parameter model. This is achieved by separating the delay imposed by the transport process from the remaining dynamics. This separation allows for a straight-forward computation of the inflow temperature from a given desired output temperature of the pipe. Applicability of the presented approach is shown by means of simulation studies and experimental results. Moreover, the feasibility of the presented control approach is proven by a spectrum analysis of the involved system operators.

As discussed in Section 4.2 the overall control structure comprises a subordinated temperature controller, which is not emphasized within the current contribution. However, as Fig. 4 shows, the desired input temperature cannot be exactly tracked by the present heater controller. Therefore, a more sophisticated control strategy for the heater has to be developed. This can be achieved by combining the presented approach with the ideas proposed in Laroche et al. (2000) and Lynch and Rudolph (2002) for a heated rod. Moreover, the extension to the variable flow case will be addressed in forthcoming research. Furthermore, in order to improve existing control strategies, the application of the presented algorithm to cooling loop networks and catalysts will be elaborated on. In addition, the underlying DPDE model shall be used for observers aimed to estimate the spatially distributed temperature profile. Such observers are of particular interest in catalyst control applications. Finally, the model may serve as the basis for the development of diagnosis and fault detection algorithms in the spirit of Fischer and Deutscher (2018).

ACKNOWLEDGEMENTS

The present contribution is a result of the research project MoReNe (FFG-Nr. 864725) funded by the Austrian Research Promotion Agency (FFG) and INNIO Jenbacher GmbH & Co OG located in Jenbach (Austria).

REFERENCES

- Bachler, S., Huber, J., Kopecek, H., and Woittennek, F. (2017a). Control of cooling loops with large and variable delays. *1st IEEE Conference on Control Technology and Applications*.
- Bachler, S., Huber, J., and Woittennek, F. (2017b). Zur thermischen Modellierung inkompressibler Rohrströmungen. *at-Automatisierungstechnik*, 65(8).
- Baehr, H.D. and Stephan, K. (2011). *Heat and Mass Transfer*. Springer Science + Business Media.
- Courant, R. and Hilbert, D. (1962). *Methods of Mathematical Physics II*. Methods of Mathematical Physics. Interscience Publishers.
- Curtain, R.F. and Zwart, H. (1995). *An Introduction to Infinite-Dimensional Linear Systems Theory*. Springer New York.
- Engel, K.J. (1999). *One-Parameter Semigroups for Linear Evolution Equations (Graduate Texts in Mathematics)*. Springer New York.
- Fischer, F. and Deutscher, J. (2018). Modulating function based fault detection for parabolic systems with polynomial faults. In *IFAC-PapersOnLine*, volume 51.
- Jie, P., Tian, Z., Yuan, S., and Zhu, N. (2012). Modeling the dynamic characteristics of a district heating network. *Energy*, 39(1), 126–134.
- John, F. (1991). *Partial Differential Equations*. Applied Mathematical Sciences. Springer New York.
- Laroche, B., Martin, P., and Rouchon, P. (2000). Motion planning for the heat equation. *International Journal of Robust Nonlinear Control*, 10, 629–643.
- Lemos, J.M. (2006). Adaptive control of distributed collector solar fields. *International Journal of System Science*, 37(8), 523–533.
- Lepreux, O. (2009). *Model-based Temperature Control of a Diesel Oxidation Catalyst*. Ph.D. thesis, École Nationale Supérieure des Mines de Paris.
- Lepreux, O., Creff, Y., and Petit, N. (2008). Motion planning for a diesel oxidation catalyst outlet temperature. *2008 American Control Conference*, 2092–2098.
- Lynch, A.F. and Rudolph, J. (2002). Flatness-based boundary control of a class of quasilinear parabolic distributed parameter systems. *International Journal of Control*, 75, 1219–1230.
- Pazy, A. (1983). *Semigroups of Linear Operators and Applications to Partial Differential Equations*. Springer New York.
- Santos, T.L., Roca, L., Guzman, J.L., Normey-Rico, J.E., and Berenguel, M. (2011). Practical MPC with robust dead-time compensation applied to a solar desalination plant. *IFAC Proceedings Volumes*, 44(1), 4909–4914.
- Smith, J.M. (1957). Closer control of loops with dead time. *Chemical Engineering Progress*, 53(5), 217–219.
- Wurm, J., Bachler, S., and Woittennek, F. (2020). On delay partial differential and delay differential thermal models for variable pipe flow. *International Journal of Heat and Mass Transfer*, 152, 119403.